GlueX-doc-2529
SVN: docs/GlueXdoc/APD_test
DRAFT: June 26, 2014

First Look at APD Samples

S. Gryba, E.S. Smith, L. Teigrob

1 Introduction

We have proposed an experiment to run in Hall D to measure rare decays of η mesons [1]. This experiment requires a calorimeter with higher resolution than the forward calorimeter that forms part of the base equipment for Hall D. The proposal is to build the new calorimeter using lead tungstate ($PbWO_4$) using the experience gained from the PRIMEX experiment [2]. The inner region of the PRIMEX hybrid calorimeter consisted of lead tungstate crystals that were $20.5 \times 20.5 \times 180$ mm^3. The light yield of the crystal demands a significant gain amplification by the combined light sensor and amplifier.

Several light sensors are under discussion to detect the scintillator light of the new calorimeter. The light of the PRIMEX calorimeter was detected using standard vacuum photomultiplier tubes. However, the magnetic fields at the location of the new calorimeter in Hall D may require more shielding than can fit into the limited space in that design. Therefore, other options for the light sensors are being considered. Avalanche Photo-Diodes (APDs) [3] are an option due to their compact size and insensitivity to magnetic fields. Some samples of these sensors are tested in this study.

2 Samples

We have investigated the response of three samples, whose properties are given in Table 1. The first two are standard S8664-1010 (square 10×10 mm^2) APDs from Hamamatsu. The third unit (rectangular 6.8×14 mm^2) comes from samples produced for PANDA [4, 5] [1].

3 Test setup

The APD samples were measured using the test apparatus setup for the HPS experiment at JLab [6]. The test setup and software were developed and documented at the University of Rome "Tor Vergata" [7] for benchmarking the large area APD (LAAPD) devices for the CLAS12 Forward Tagger (FT) calorimeter. The test apparatus was reproduced at JLab for testing similar devices for the HPS experiment **??**, which will run in Hall B.

[1] Kindly loaned to us by Ulrike Thoma and Werner Erni.

Table 1: Table of properties of two square APD samples. The properties were provided by Hamamatsu at 25°C with a light source of $\lambda = 420$nm.

Type	Serial No.	V_{br} (V)	V_{oper} (V) (Gain=50)	I_{oper} (nA) (Gain=50)
S8664-1010	AA4654	415	366.9	16
S8664-1010	AA4655	419	370.8	14

For completeness, we include here a description of the setup and measurements. The apparatus allows two groups of 12 LAAPDs to be tested at the same time at predefined, fixed temperatures. The characterization of the LAAPD is performed by measuring the currents across the device when a supply voltage V is applied both in light and dark conditions. A programable micro-chiller (Lauda model RC20S) provides refrigeration that cools two copper plates that maintain the sensors at predefined temperatures between 22 and -6°C. The actual temperature of the copper plates is measured using two PT100 resistance temperature detectors (RTDs). The sensors are illuminated using a blue LED light source, which is distributed uniformly using a reflective cup. The setup is placed in a light-tight plastic box filled with nitrogen to prevent condensation. An electrometer (Keithley model 6517A) provides stable and adjustable supply voltages to all LAAPDs and it measures the current of one channel at a time using external custom electronics. The remote control of the chiller, RTD temperature read-back, and cycling through sensor readings is accomplished via a personal computer and LabView program. More details can be found in Ref. [7].

4 Measurements

We followed the standard procedure for testing APDs for the HPS experiment. An automatic measuring sequence was specified to take data at four temperatures and cover a range of voltages up to the breakdown voltage. The breakdown and operating voltages for the S8664-1010 were provided by the manufacturer (Hamamatsu). We did not have the operating parameters for the rectangular sensor, which we denote PANDA-0714, so we used the parameters of the S8664-1010 units to establish the range of voltage measurements. The LabView program followed the predetermined sequence to take data over the specified range of voltages after the temperature had settled. Data were taken at the chiller settings of T = 25, 20, 18 and 16 °C. However, the temperature of the setup was determined from the RTD readings, which were approximately 0.7°C higher. In the following we refer to the figures for the PANDA-0714 APD, but subsequent figures show the corresponding data for the S8664-1010 APDs.

The data consists of the current measured at a fixed temperature over a range of preset voltages both with the LED on and under dark conditions (see Fig. 1 and Fig. 2). The response is then normalized to data taken in the limit of null applied

Table 2: Table of measured properties of the three APD samples, recorded at 25.55°C with a blue LED. The breakdown voltages for the first two samples are taken from the Hamamatsu data sheet.

Type	Serial No.	V_{br} (V)	V_{oper} (V) (Gain=50)	I_{oper} (nA) (Gain=50)
S8664-1010	AA4654	415	368	16
S8664-1010	AA4655	419	372	14
PANDA-0714	0605004458	∼447	400	10

voltage, which corresponds to unity gain. The extrapolation to zero voltage is accomplished using measurements from 5 to 50 volts in steps of 5 V. Coarser steps are taken over most of the voltage range, but revert to steps of 5 V or less for the operating region beyond 350 V to within 5 V of the breakdown voltage. The gain as a function of voltage at the four temperatures determined in this way is shown in Fig. 3. The measured currents are typically 10 nA at unity gain and increase to a few μA in the operating region. The dark current should be a linear function of the gain, as shown Fig. 4. The temperature readings of the RTDs during the time of measurements at each temperature setting are shown in Fig. 5. The variation is less than 0.01°C, which we ignore, and assign the measurements to the average temperature given in the figure.

In this manner we extract the gain as a function of voltage at fixed temperature, which exhibits the following linear scaling behavior

$$G(V,T) \quad = \quad G(\alpha V - \beta T). \tag{1}$$

The function of G(V,T) is inverted to obtain the voltage that must be applied to the APD to obtain a given gain at fixed temperature, namely V(G,T). The variation of the normalized gain with voltage ($\frac{1}{G}\frac{dG}{dV}$) is shown in Fig. 7 and has a shape independent of temperature as demonstrated in Fig. 8, where the data from all four temperatures are superimposed. Of interest is also the voltage dependence on temperature at fixed gain. See Fig. 9 that plots the data points of temperature vs. voltage extrapolated to a fixed gain. Finally, the gain as a function of voltage in the operating region is plotted in Fig. 10 at the four different temperatures.

5 Summary and conclusions

The samples that we tested were well-behaved. We confirmed the properties of the two S8664-1010 APDs as detailed in the Hamamatsu data sheet. We did not have the data sheet for the PANDA-0714, but its performance was very similar although the breakdown voltage was about 30 V higher. The gains for the S8664-1010 are shown in Fig. 31, where the AA4654 voltage was shifted up by 4 V to match the breakdown voltage of the AA4655. The curves lie almost right on top of one another, which

shows that their response in the operating region are the same when the voltages are measured relative to the breakdown point. The comparison of gain curves for the PANDA-0714 and AA4655 is shown in Fig. 32. The voltages from the PANDA-0714 were shifted down by 28 V for the gain curves to match. Again we see that the the APD response is very similar if voltages are measured relative to the breakdown voltage.

We also determined the voltage and dark current for a gain of 50 to compare with the Hamamatsu data sheet (see Table 2). The voltage settings determined for a gain of 50 are 368 V for the AA4654 and 372 V for the AA4655 at 25.55 °C, 1.2 V higher than those specified by Hamamatsu at 25 °C. A complete propagation of uncertainties has not been performed including interpolation, but it is likely that these differences are within the experimental errors. The measured dark current for AA4654 was 16 nA and for AA4655 it was 14 nA, consistent with the data from Hamamatsu. The dark current for the PANDA-0714 unit was 10 nA. We conclude that the behavior of the square and rectangular APDs is very similar, although the operating voltage for the rectangular APD is about 30 V higher.

6 Acknowlegements

We would like to thank Michel Garçon and the HPS experiment for providing access to the APD test setup. In addition, we would like to acknowledge Holly Vance and Volodymyr Iurasov, who collected the data and provided the software tools to analyze them.

References

[1] JLab-Proposal-13-004. Symmetry Tests of Rare Eta Decays to All-Neutral Final States: The JLab Eta Factory (JEF) Experiment. L. Gan, contact person, 2013. 1

[2] I. Larin et al. A New Measurement of the π^0 Radiative Decay Width. *Phys.Rev.Lett.*, 106:162303, 2011. 1

[3] Hamamatsu Corporation. Opto-semiconductor handbook. *Chapter 2: Si photodiodes*, http://www.hamamatsu.com/sp/ssd/doc_en.html. 1

[4] PANDA Collaboration. AntiProton Annihilations at Darmstadt. http://www-panda.gsi.de/. 1

[5] PANDA Collaboration. Technical Design Report for PANDA Electromagnetic Calorimeter. http://www-panda.gsi.de/html/det/emc/tdr/panda_tdr_EMC.pdf. 1

[6] HPS Collaboration. Heavy Photon Search at Jefferson Laboratory. C12-11-006, J. Jaros, contact person. https://misportal.jlab.org/mis/physics/experiments/viewProposal.cfm?paperId=738. 1

[7] Rizzo, A. *et al.* Report on Forward Tagger LAAPD Benchmarking. Description of the procedure used to determine the gain, dark rate and stability of 380 LAAPDs at various temperatures to be used for the CLAS12 Forward Tagger (FT) Calorimeter., March 2014. 1, 2

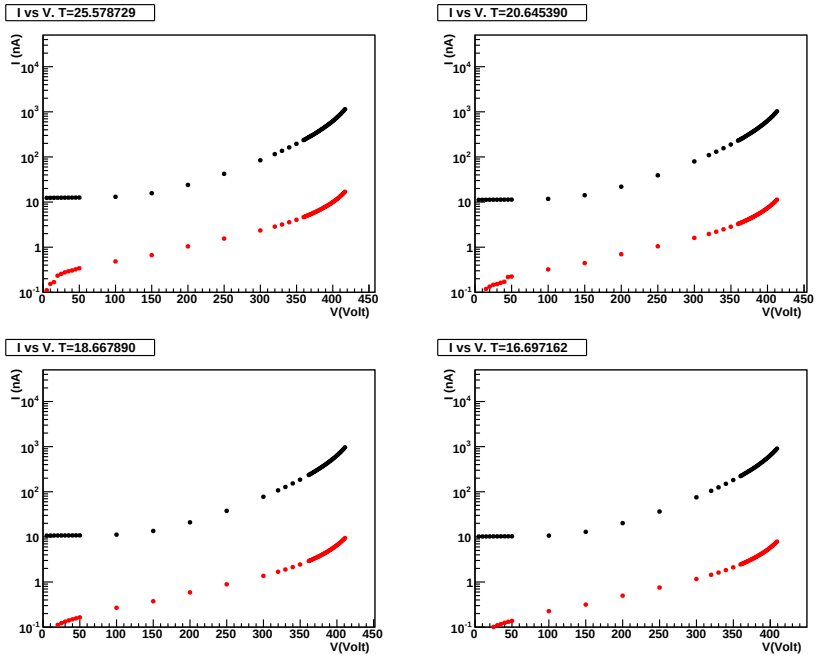

Figure 1: APD 0605004458. Current and dark current vs voltage at four different temperatures.

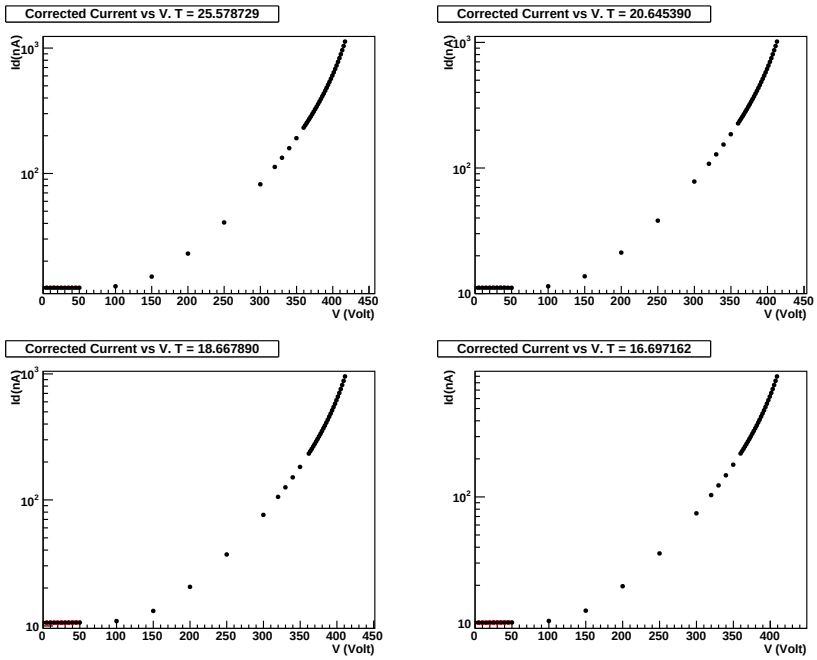

Figure 2: APD 0605004458. Current - dark current vs voltage at four different temperatures.

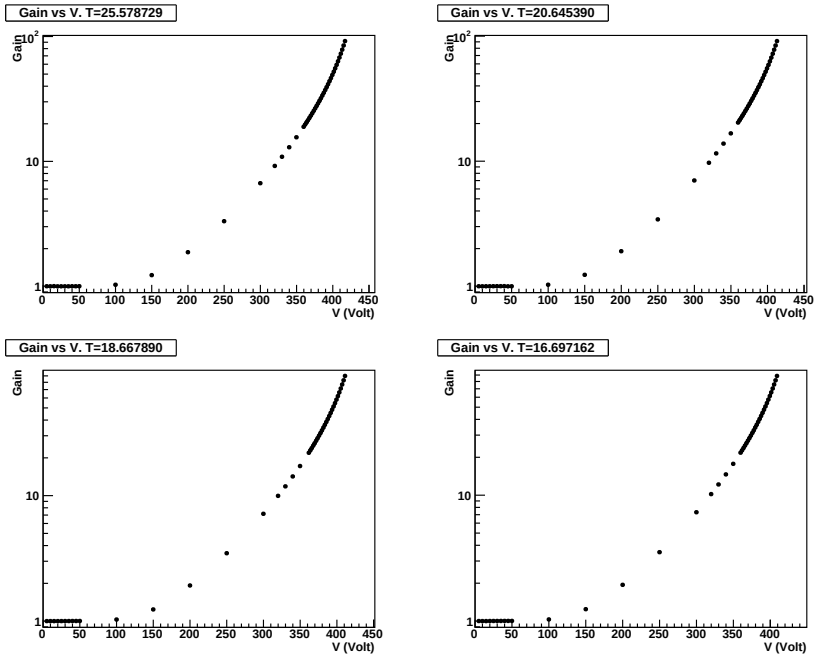

Figure 3: APD 0605004458. Gain vs voltage at four different temperatures.

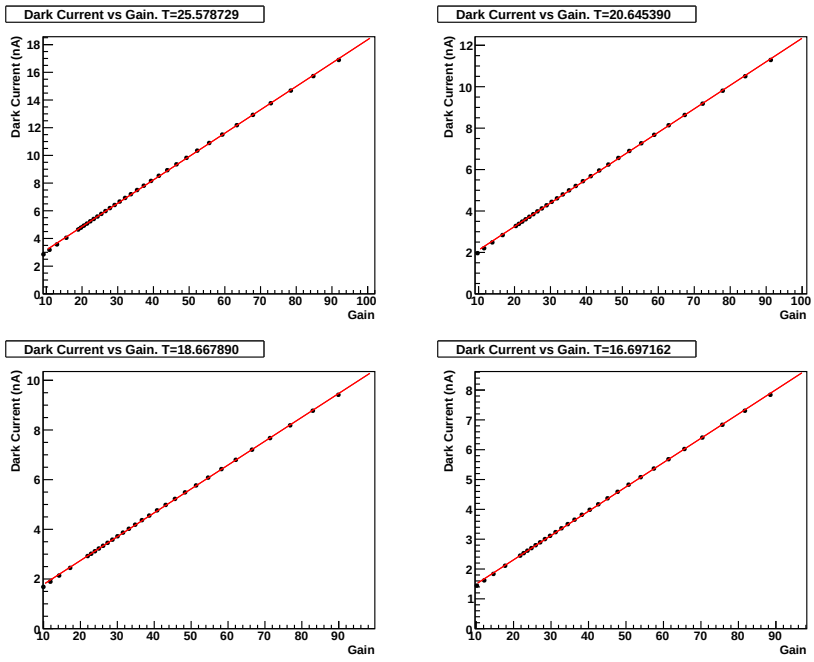

Figure 4: APD 0605004458. Dark current vs gain at four different temperatures.

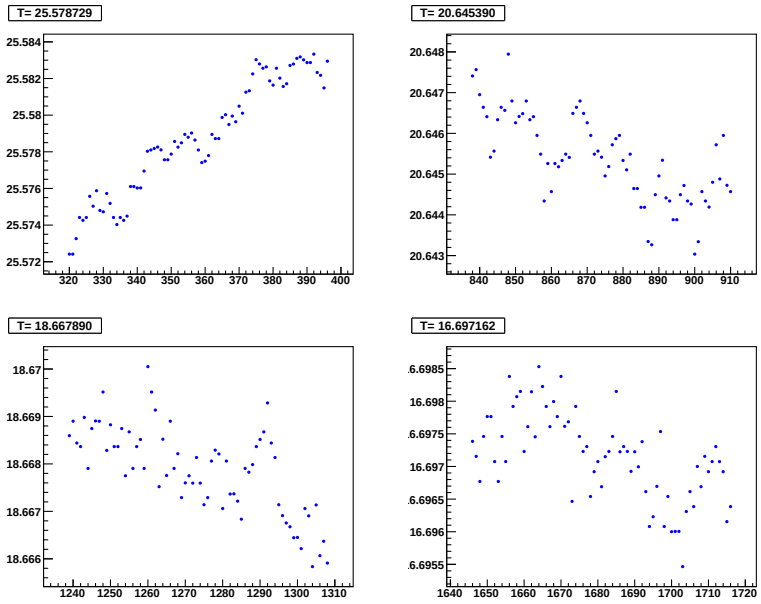

Figure 5: APD 0605004458. Measured temperatures vs voltage setting. The average temperature is indicated in the box.

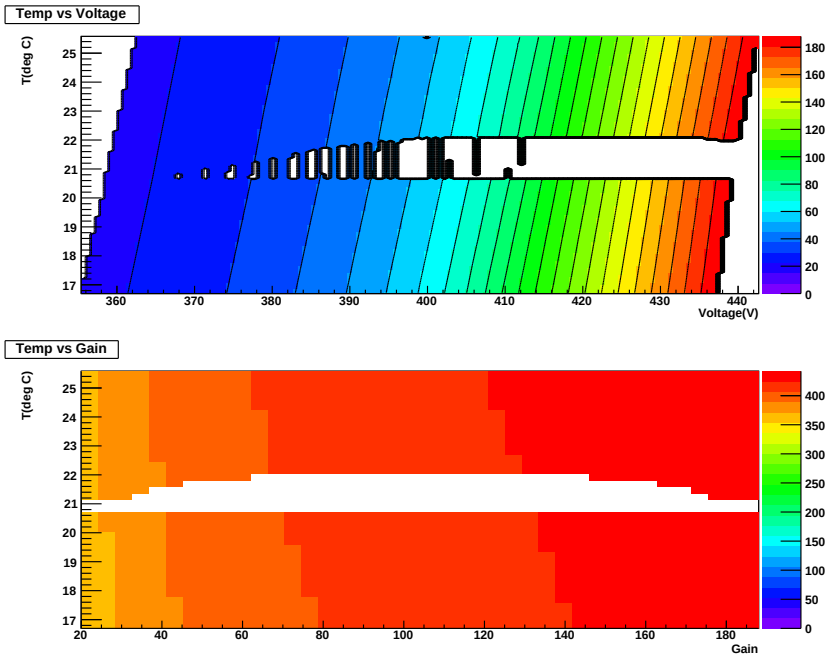

Figure 6: APD 0605004458. Top) Gain as a function of temperature and voltage. Bottom) Voltage as a function of temperature and gain. Blank regions correspond to areas where data coverage is poor.

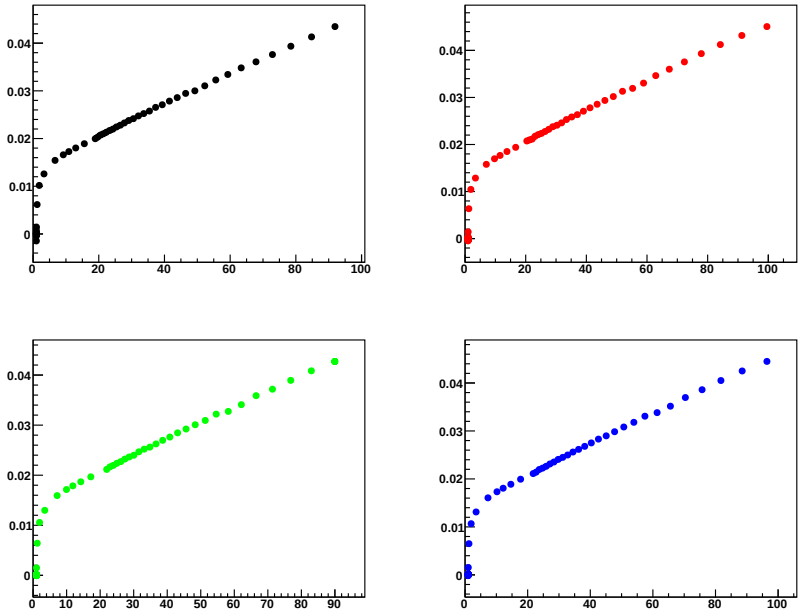

Figure 7: APD 0605004458. $(\frac{1}{G}\frac{dG}{dV})$ [V^{-1}] vs G at four different temperatures.

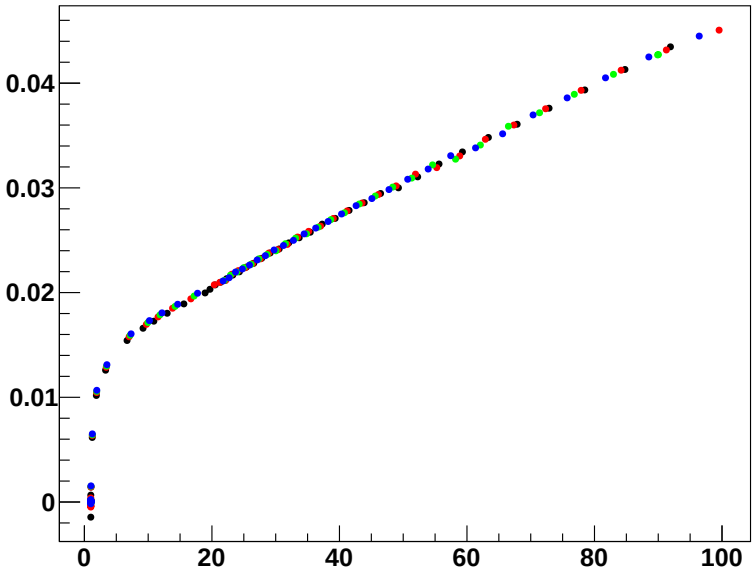

Figure 8: APD 0605004458. $(\frac{1}{G}\frac{dG}{dV})$ [V^{-1}] vs G with four temperatures superimposed.

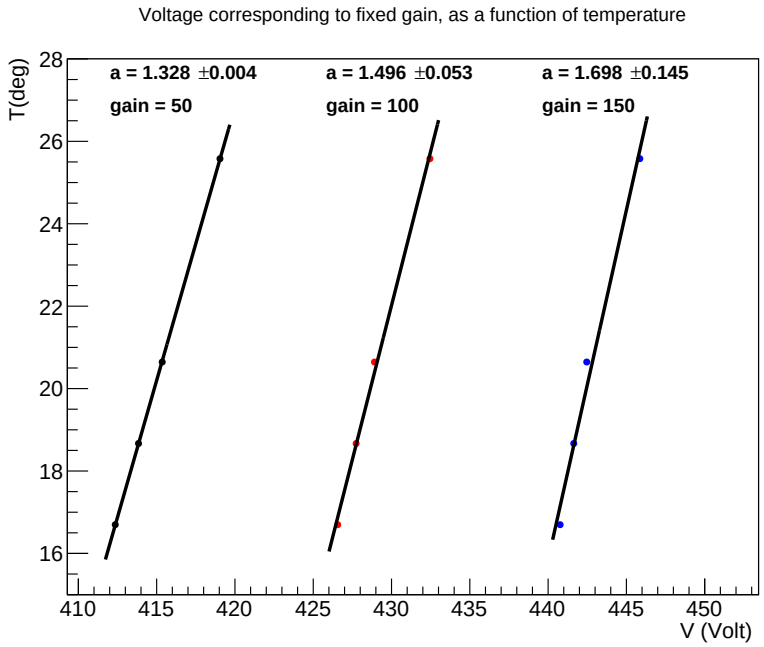

Figure 9: APD 0605004458. Temperature vs voltage at fixed gain. The fits at gain=100,150 extrapolate beyond the range of the data.

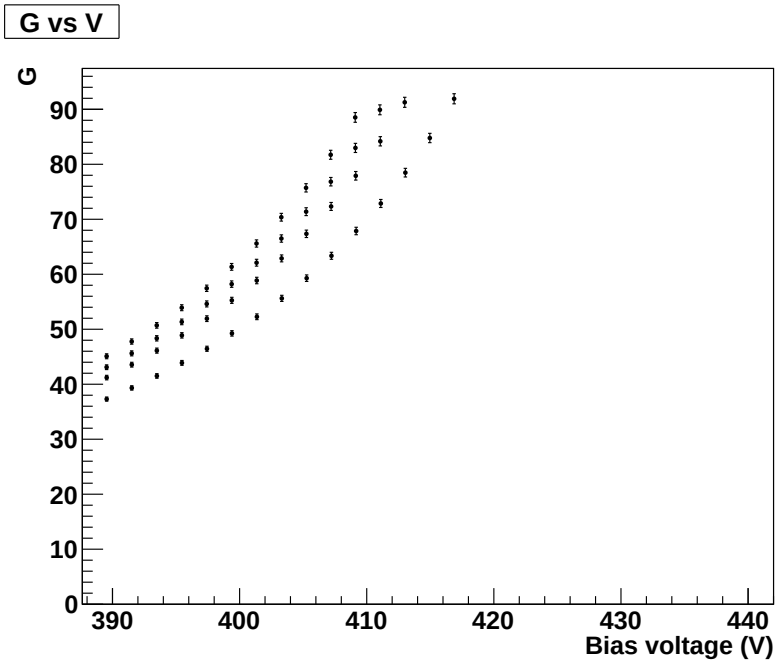

Figure 10: APD 0605004458. Gain vs voltage at four different temperatures.

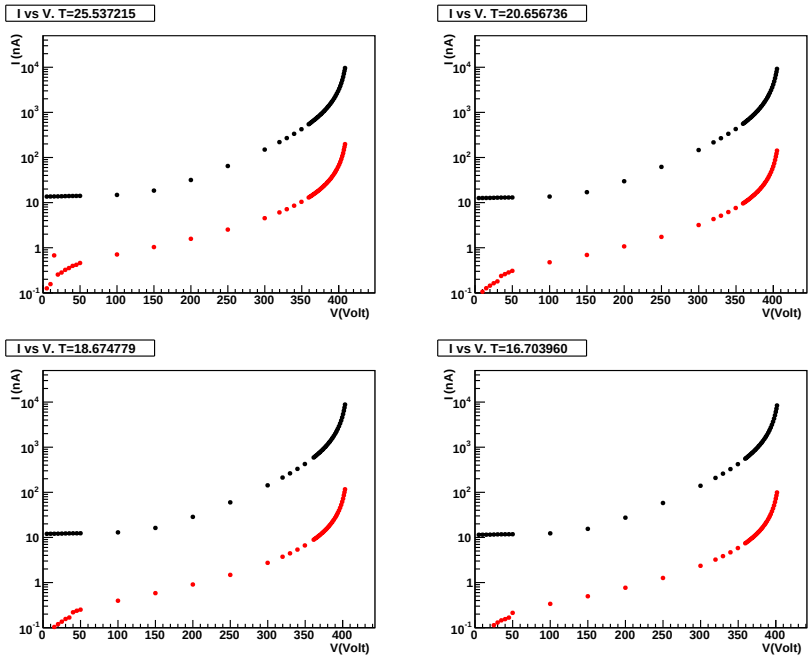

Figure 11: APD AA4654. Current and dark current vs voltage at four different temperatures.

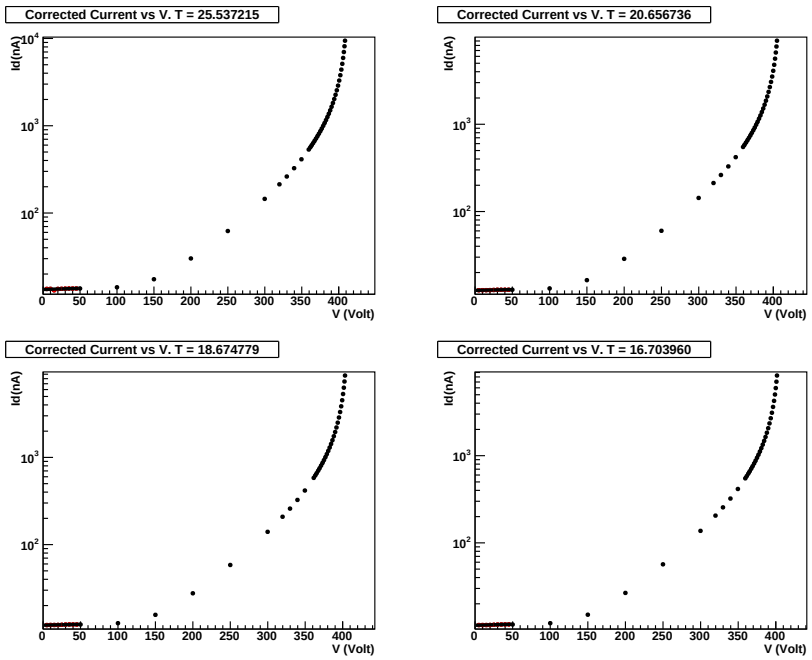

Figure 12: APD AA4654. Current - dark current vs voltage at four different temperatures.

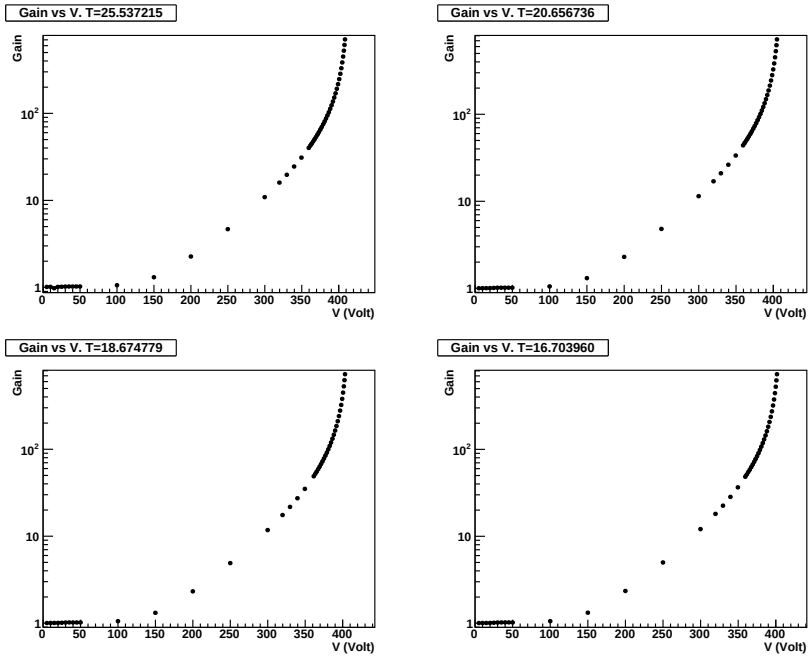

Figure 13: APD AA4654. Gain vs voltage at four different temperatures.

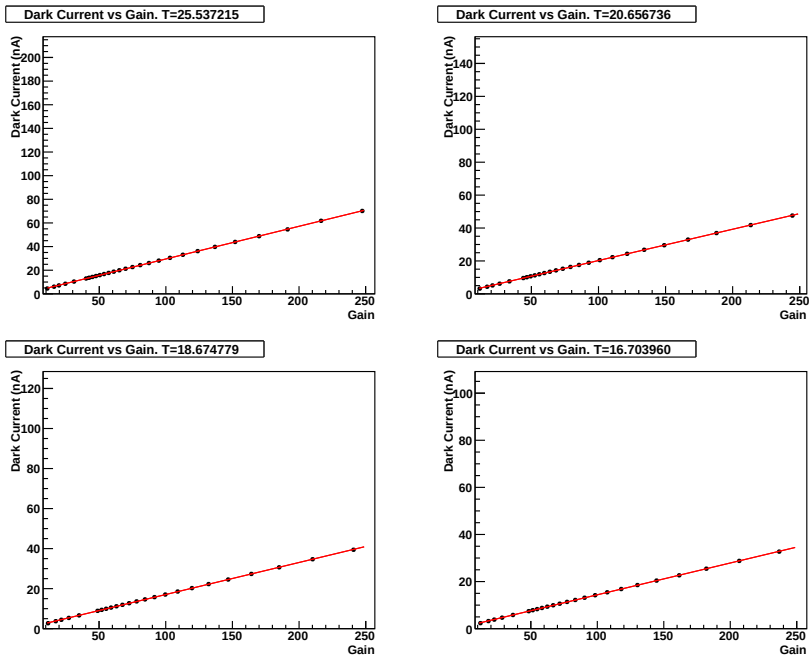

Figure 14: APD AA4654. Dark current vs gain at four different temperatures.

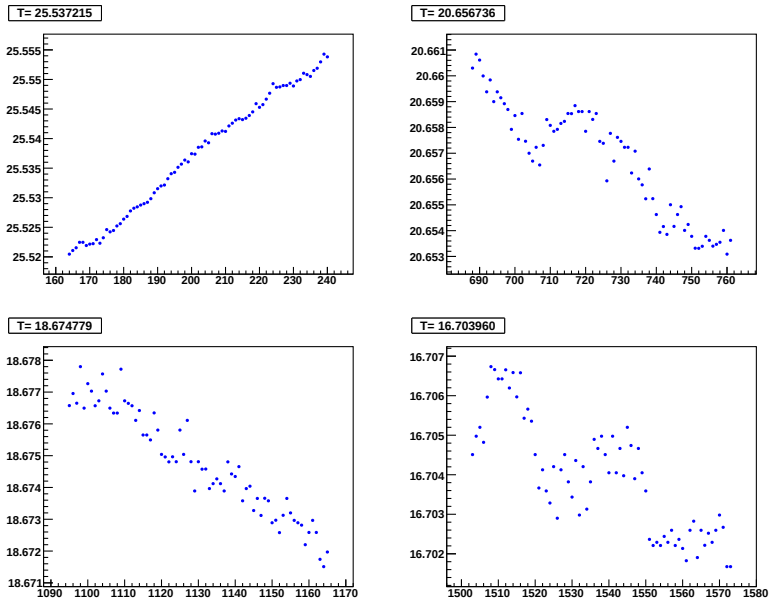

Figure 15: APD AA4654. Measured temperatures vs voltage setting. The average temperature is indicated in the box.

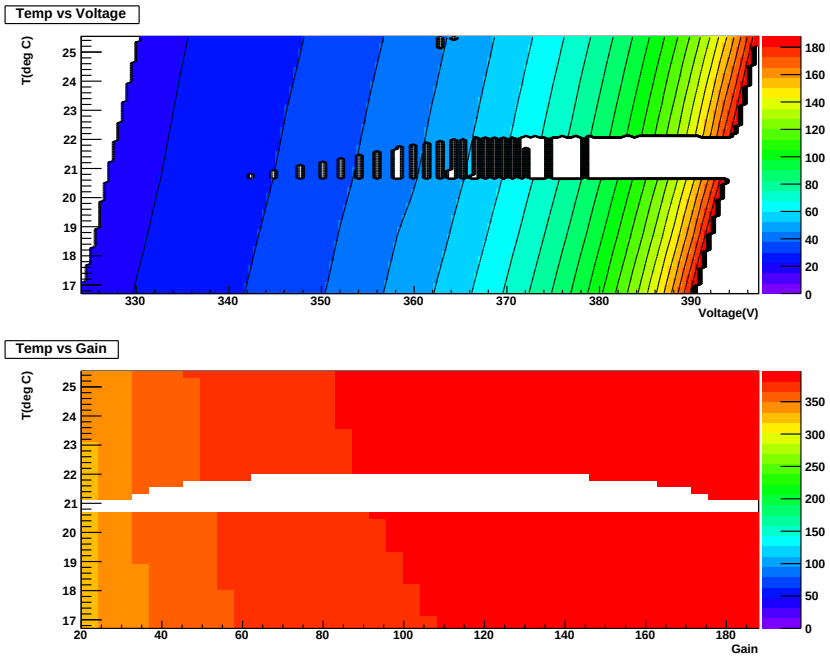

Figure 16: APD AA4654. Top) Gain as a function of temperature and voltage. Bottom) Voltage as a function of temperature and gain. Blank regions correspond to areas where data coverage is poor.

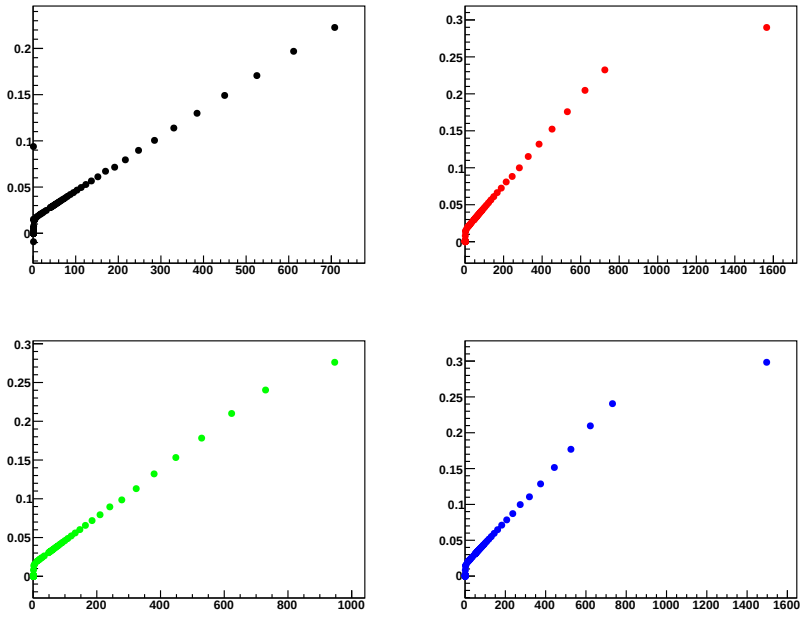

Figure 17: APD AA4654. $(\frac{1}{G}\frac{dG}{dV})$ [V^{-1}] vs G at four different temperatures.

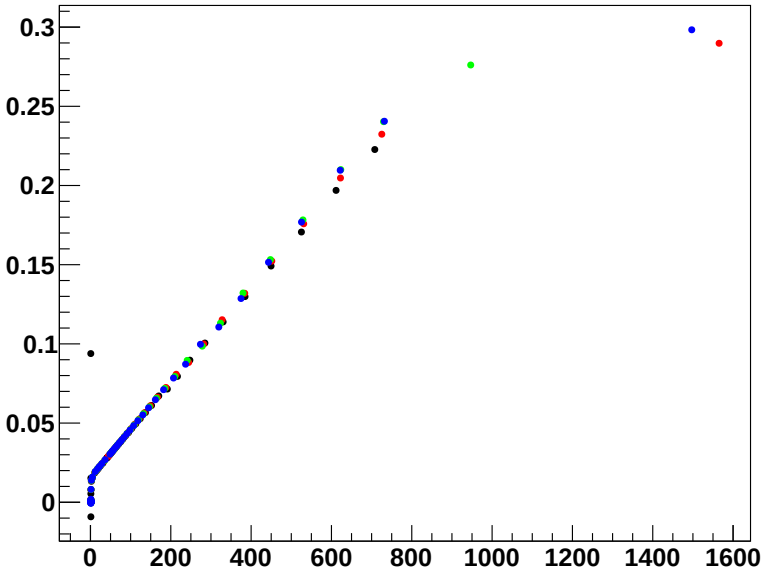

Figure 18: APD AA4654. $(\frac{1}{G}\frac{dG}{dV})$ [V^{-1}] vs G with four temperatures superimposed.

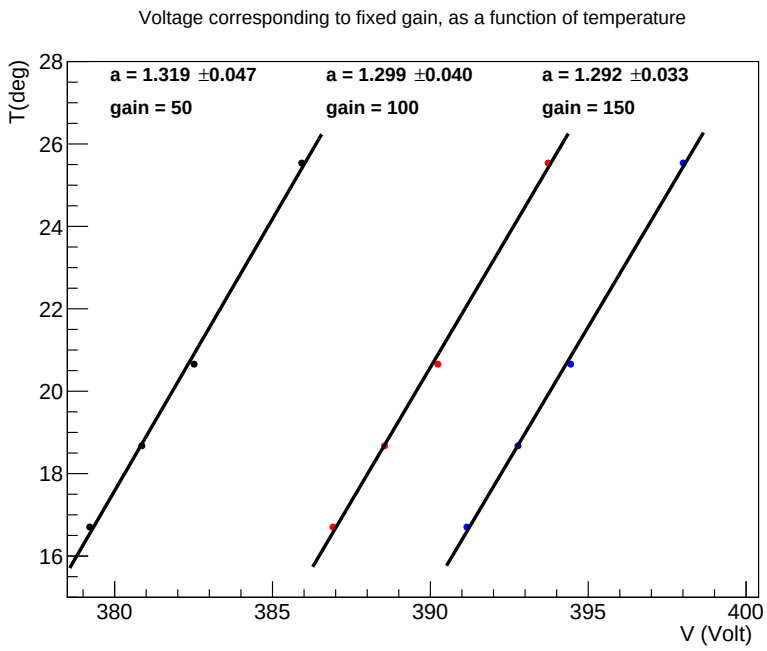

Figure 19: APD AA4654. Temperature vs voltage at fixed gain

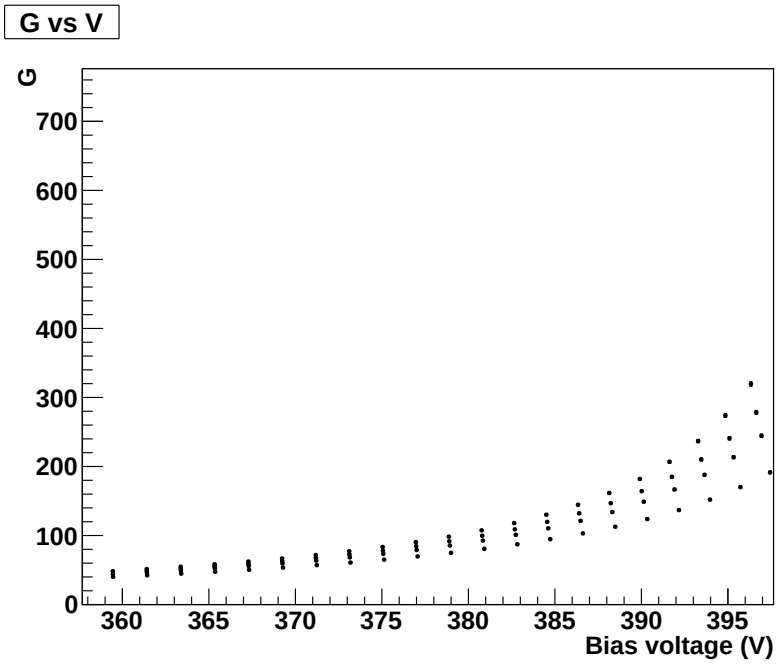

Figure 20: APD AA4654. Gain vs voltage at four different temperatures.

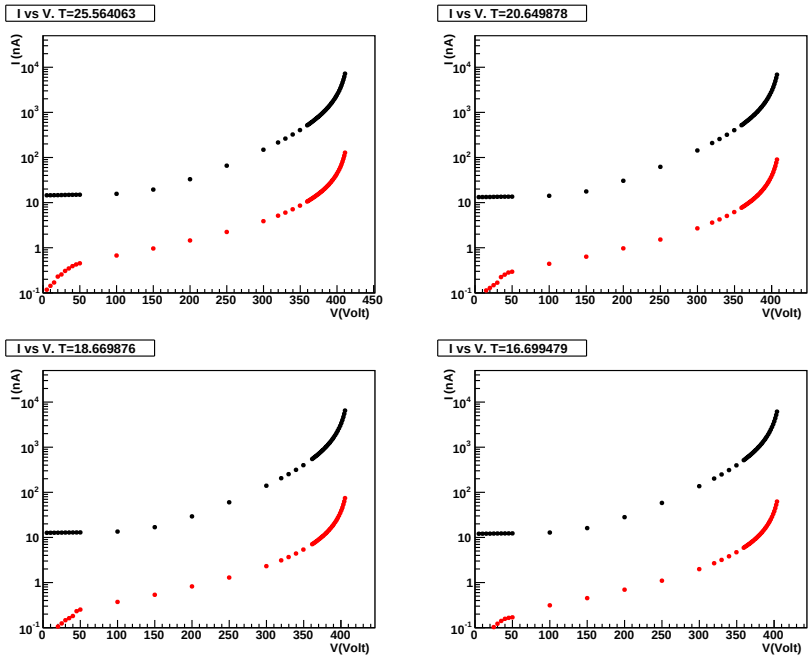

Figure 21: APD AA4655. Current and dark current vs voltage at four different temperatures.

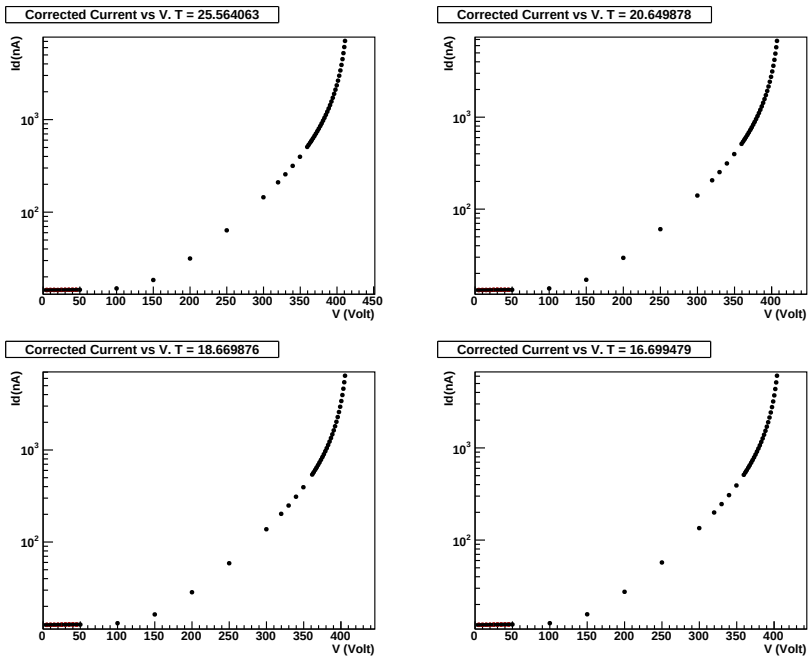

Figure 22: APD AA4655. Current - dark current vs voltage at four different temperatures.

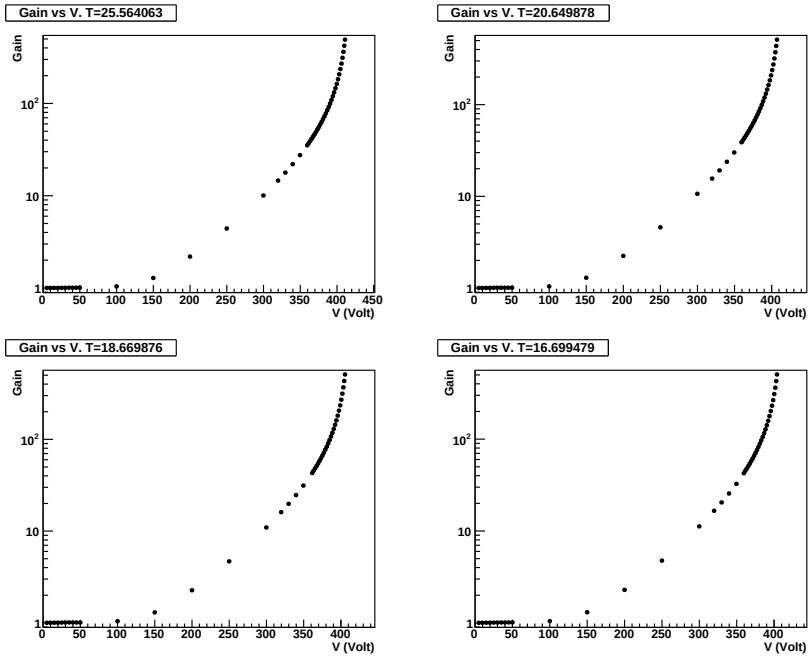

Figure 23: APD AA4655. Gain vs voltage at four different temperatures.

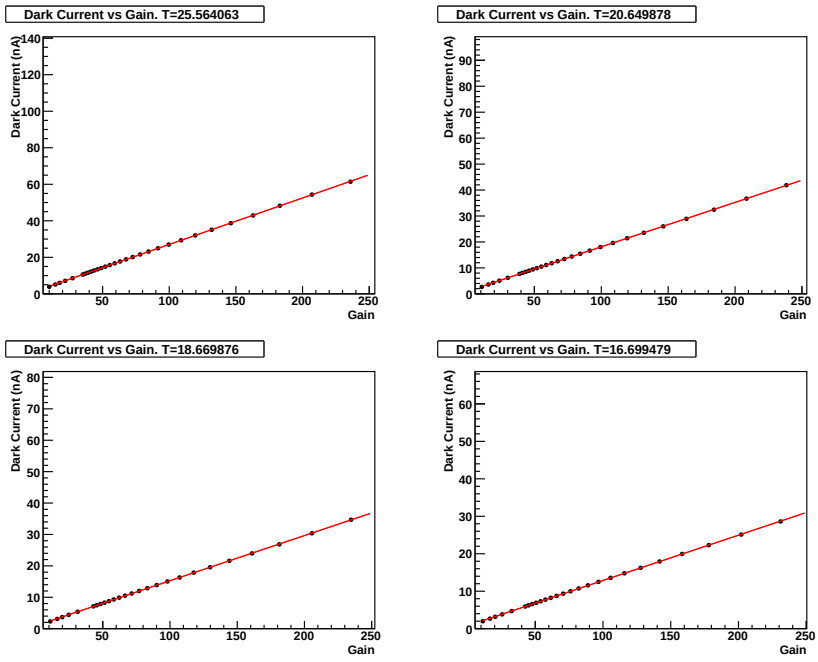

Figure 24: APD AA4655. Dark current vs gain at four different temperatures.

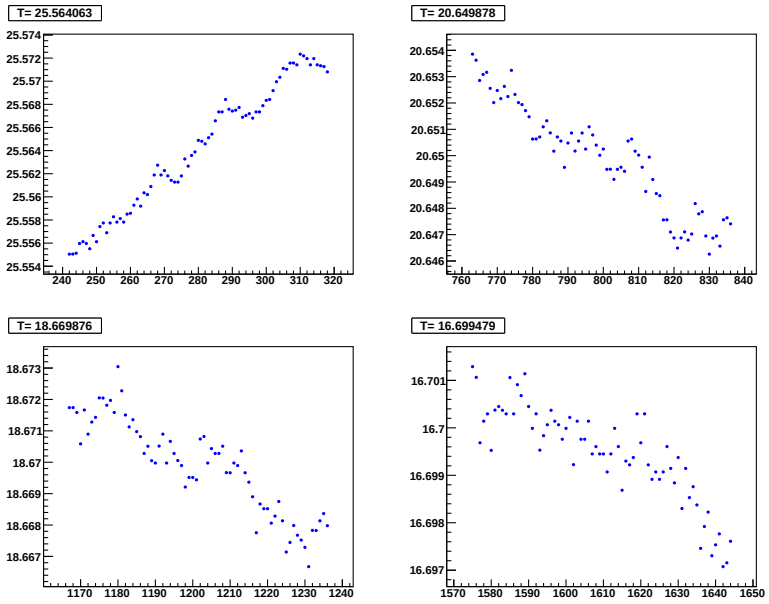

Figure 25: APD AA4655. Measured temperatures vs voltage setting. The average temperature is indicated in the box.

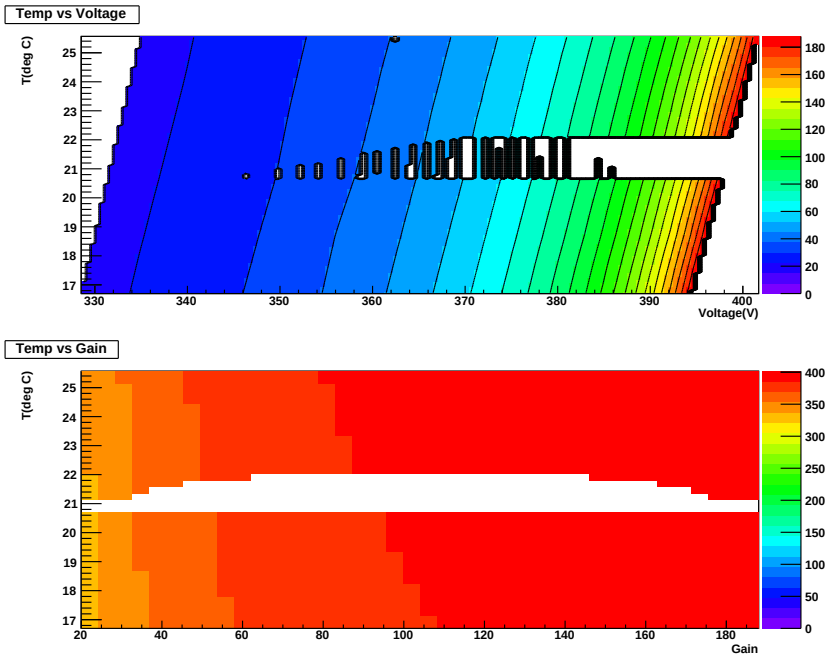

Figure 26: APD AA4655. Top) Gain as a function of temperature and voltage. Bottom) Voltage as a function of temperature and gain. Blank regions correspond to areas where data coverage is poor.

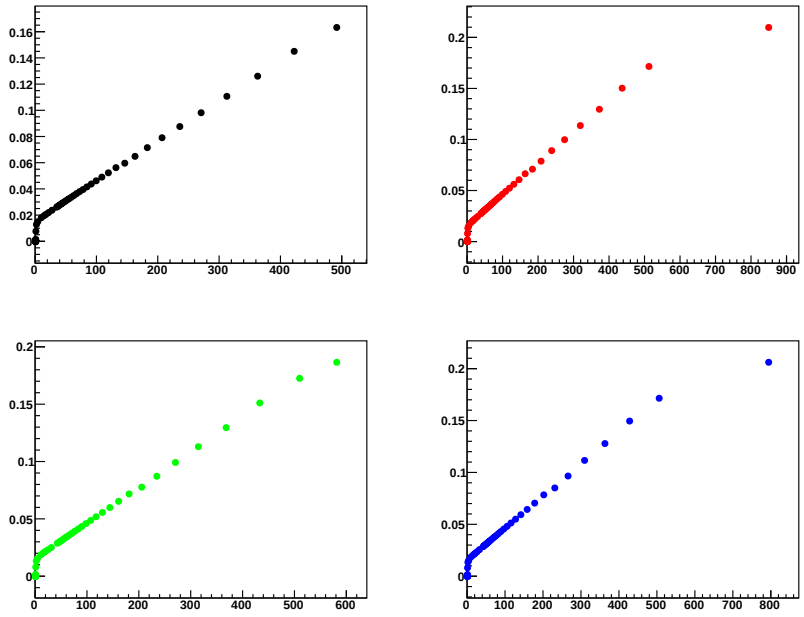

Figure 27: APD AA4655. $(\frac{1}{G}\frac{dG}{dV})$ [V^{-1}] vs G at four different temperatures.

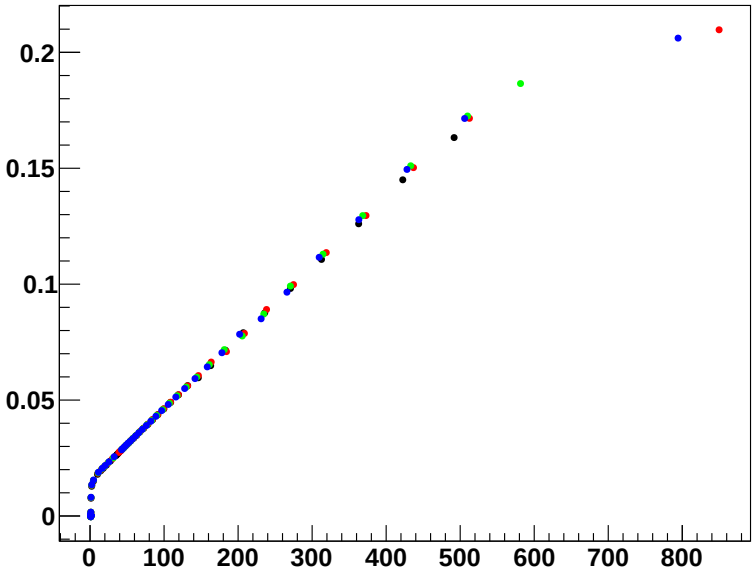

Figure 28: APD AA4655. $(\frac{1}{G}\frac{dG}{dV})$ [V^{-1}] vs G with four temperatures superimposed.

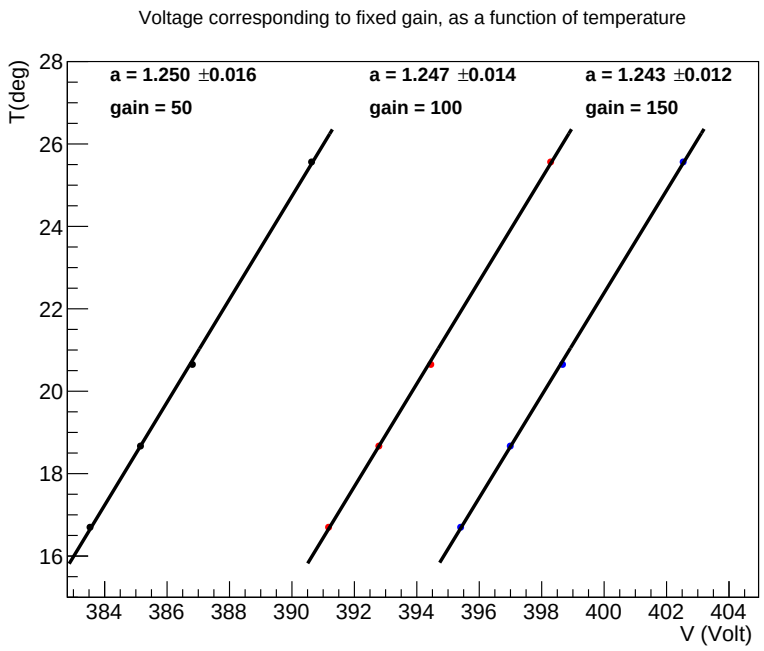

Figure 29: APD AA4655. Temperature vs voltage at fixed gain

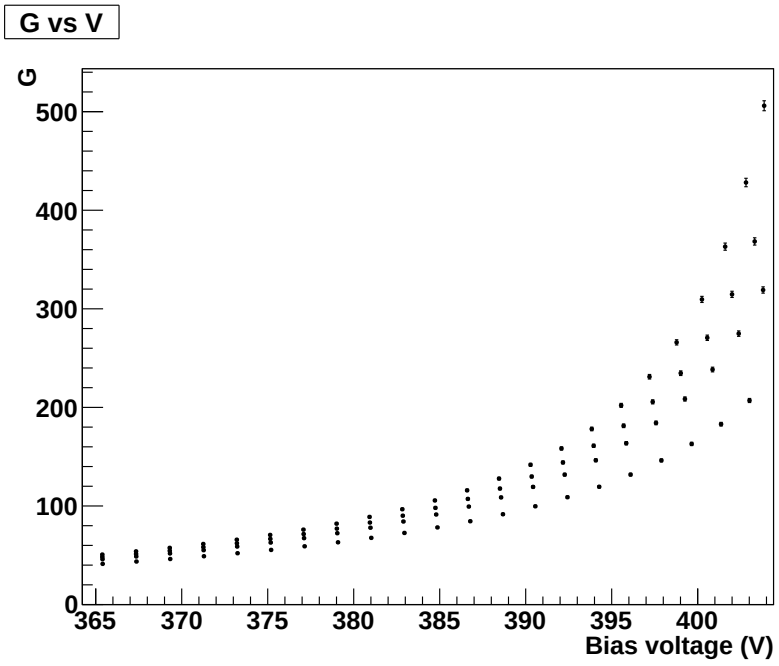

Figure 30: APD AA4655. Gain vs voltage at four different temperatures.

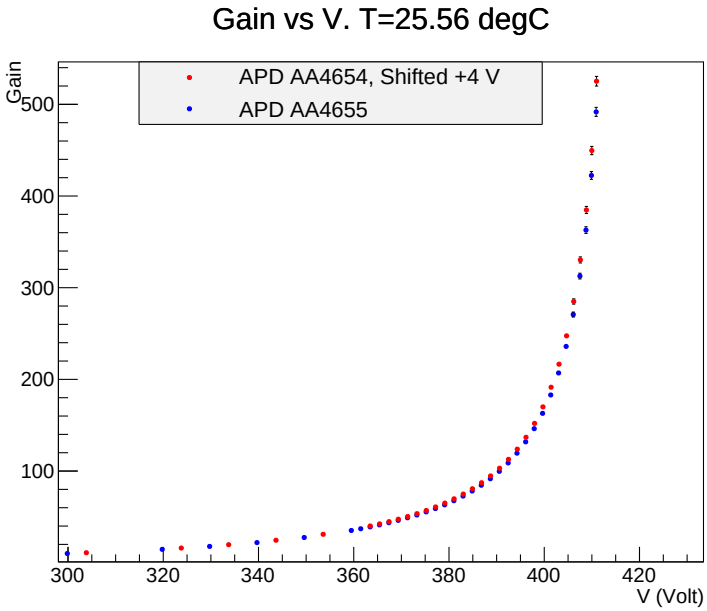

Figure 31: Gain curves for the two S8664-1010 APDs, AA4654 and AA4655, are overlaid. The voltage settings for the AA4654 are shifted higher by 4 V to compensate for the different breakdown voltage.

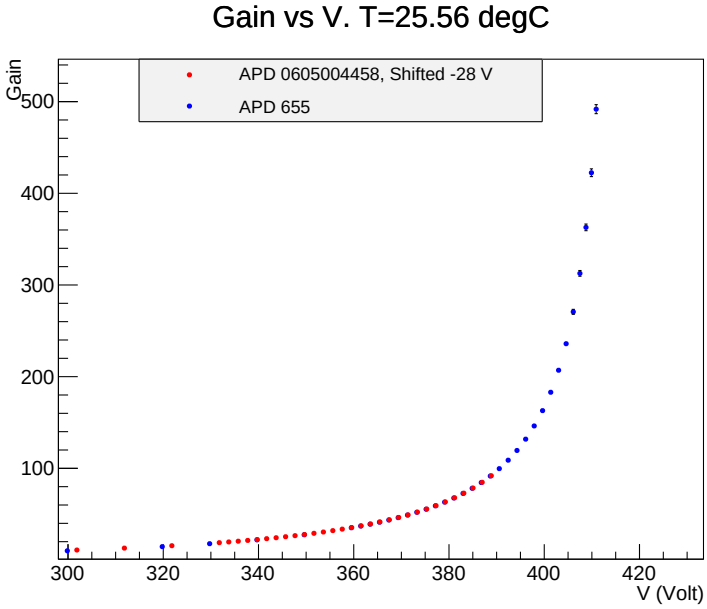

Figure 32: Gain curves for PANDA-0710 0605004458 and S8664-1010 AA4655 are overlaid. The voltage settings for the PANDA-0710 are shifted lower by 28 V to visually match the data for the S8664-1010.